

Robust Global Synchronization of a Hyperchaotic System with Wide Parameter Space via Integral Sliding Mode Control Technique

Edwin A. Umoh ^{a,1,*}, Omokhafa J. Tola ^{b,2}

^a Department of Electrical and Electronic Engineering Technology, Federal Polytechnic, Kaura Namoda, Nigeria

^b Department of Electrical and Electronic Engineering, Federal University of Technology, Minna, Nigeria

¹ eddyumoh@gmail.com; ² omokhafa@gmail.com

* Corresponding Author

ARTICLE INFO

Article history

Received 20 October 2021

Revised 28 October 2021

Accepted 31 October 2021

Keywords

Hyperchaotic system;

Lyapunov stability theory;

Integral sliding mode control;

Synchronization

ABSTRACT

The inherent property of invariance to structural and parametric uncertainties in sliding mode control makes it an attractive control strategy for chaotic dynamics control. This property can effectively constrain the chaotic property of sensitive dependence on initial conditions. In this paper, the trajectories of two identical four-dimensional hyperchaotic systems with fully-known parameters are globally synchronized using the integral sliding mode control technique. Based on the exponential reaching law and the Lyapunov stability principle, the problem of synchronizing the trajectories of the two systems was reduced to the control objective of asymptotically stabilizing the synchronization error state dynamics of the coupled systems in the sense of Lyapunov. To verify the effectiveness of the control laws, the model was numerically tested on a hyperchaotic system with a wide parameter space in a master-slave configuration. The parameters of the hyperchaotic system were subsequently varied to evolve a topologically non-equivalent hyperchaotic system that was identically coupled. In both cases, the modeled ISM control laws globally synchronized the dynamics of the coupled systems after transient times, which sufficiently proved the invariance property of the ISMC. This study offers an elegant technique for the modeling of an ISMC for hyperchaotic coupling systems. As an open problem, this synchronization technique holds promises for applications in robot motion control, chaos-based secure communication system design, and other sensitive nonlinear system control.

This is an open-access article under the [CC-BY-SA](https://creativecommons.org/licenses/by-sa/4.0/) license.



1. Introduction

Chaotic systems have played a crucial role in the understanding of phenomena that governed the development of science and technology. During the last three decades, intensive research into chaos has resulted in a deeper understanding of the interactions between physical, biological, economic, physiological, and social sciences. The plethora of literature has convincingly demonstrated the applications of chaos in various disciplines, including

economics, medicine, finances, security studies, telecommunications. Chaos theory has been applied to robotics. As the understanding of chaos deepens, higher dimension chaotic systems have been evolved, even as the frontiers of applications and hypotheses expanded considerably over the last three decades. Essentially, in order to be useful, chaos must be controlled. Thus, various control techniques have been applied to the control and synchronization of chaos. These techniques include adaptive control, fuzzy control, hybrid feedback control, backstepping control, contraction control, among others. Synchronization is very useful in telecommunication science and occurs when two chaotic systems are coupled such that, in spite of the exponential divergence of their nearby trajectories, synchrony of the trajectories is still achieved as $t \rightarrow \infty$, provided conditions related to the coupling strength, parameter region of the systems are satisfied, in addition to satisfying a necessary condition for master-slave synchronization which is that the non-driven slave subsystem must be asymptotically stable in the sense of Lyapunov [1].

Sliding mode control (SMC) has emerged as a robust control technique for systems constraint by uncertainties and unpredictability. SMC is a control technique that is based on the design of switching laws to drive system trajectories to a user-chosen hyperplane in the state space [2]. It is attractive due to its property of invariance to parametric and non-parametric uncertainties. The global response of SMC consists of two phases known as the reaching phase and the sliding phase. In the reaching phase, the system's states are constrained to reach a predetermined sliding surface in finite time. On this surface, the controlled system is adaptively altered to a sliding mode, resulting in the system sliding towards the origin along the sliding surface for a duration known as the sliding phase [3].

SMC has been applied to a variety of systems, including super-switching control [4], unmanned vehicle [5], single input, multi-output systems (SIMO) [6], stepper motor control [7], machine infinite bus system [8], MIMO system [9][10], stepper motor drive system [11], two-link flexible manipulator [12], autonomous vehicle [13] and secure communication [14]. In practice, invariance cannot be guaranteed in the reaching phase. Thus, several studies have proposed some improvement in the reaching law [15]–[19]. A new SMC design known as integral SMC (ISMC) was proposed in [20]. ISMC essentially circumvents the challenges posed by the reaching phase and offers dexterous application in complex systems. In succeeding years, several researchers have applied ISMC to a variety of control problems, including the Euler-Lagrange system [21], chaos synchronization [22], two-wheel vehicle [23], underactuated rotary hook system [24].

This research contributes to the application of the ISMC technique to synchronize the dynamics of wide parameter spaced hyperchaotic systems, which are traditionally more sensitive than other hyperchaotic systems due to their large Lyapunov exponents. The rest of the paper is organized as follows: Section 2 describes the selected hyperchaotic system. Section 3 presents the design of the switching surface and integral sliding mode controller. Section 4 unveiled the numerical simulation results, while the conclusion and future work is given in Section 5.

2. Methods

In this section, the architecture of the proposed ISMC system is presented. The algebraic structure of the hyperchaotic system and its 3-D phase portrait are presented.

2.1. The architecture of the ISMC system and algebraic structure of the hyperchaotic system

The architecture of the proposed controller comprises the master and slave systems, synchronization error system, nonlinear functions (which provides the nonlinearity), and the sliding manifold on which the trajectories slide. The architecture is shown in Fig. 1.

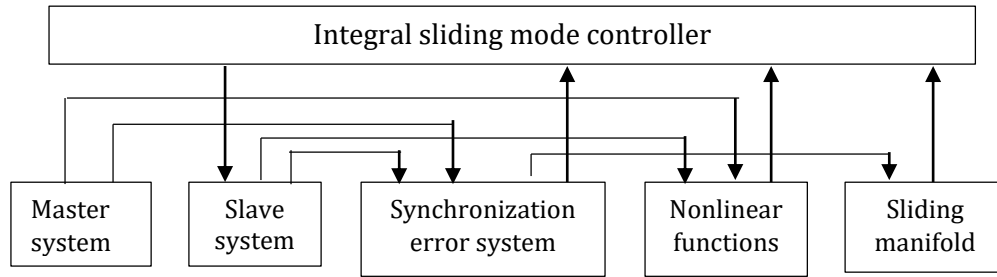


Fig. 1. The architecture of the ISMC system

The hyperchaotic system used in the study was first reported in [25]. The hyperchaotic system is well-suited for studying the robustness of integral sliding mode controllers due to its huge parameter space and unstable dynamics [26]–[29]. The algebraic structure of the system is represented by four-coupled ordinary differential equations of the form:

$$\begin{aligned}\dot{x}_1 &= -\alpha_1(x_1 + x_2) + \alpha_2x_3 \\ \dot{x}_2 &= -\alpha_3x_1x_3 + \alpha_4x_2 + \alpha_5x_4 \\ \dot{x}_3 &= \alpha_6x_1x_2 + \alpha_7 \\ \dot{x}_4 &= -\alpha_8x_1 - \alpha_9x_2 - \alpha_{10}x_3 - \alpha_{11}x_4\end{aligned}\quad (1)$$

Where $\alpha_1, \alpha_2, \alpha_3 \dots \alpha_{11}$ are system parameters and $x_1, x_2, \dots x_4$ are the state variables. When $\alpha_1 = 20, \alpha_2 = 1, \alpha_3 = 10, \alpha_4 = 5, \alpha_5 = 1, \alpha_6 = 10, \alpha_7 = 10, \alpha_8 = 0.01, \alpha_9 = 0.8, \alpha_{10} = 0.01, \alpha_{11} = 0.01$. The following time series of the state trajectories shown in Fig. 2 are generated.

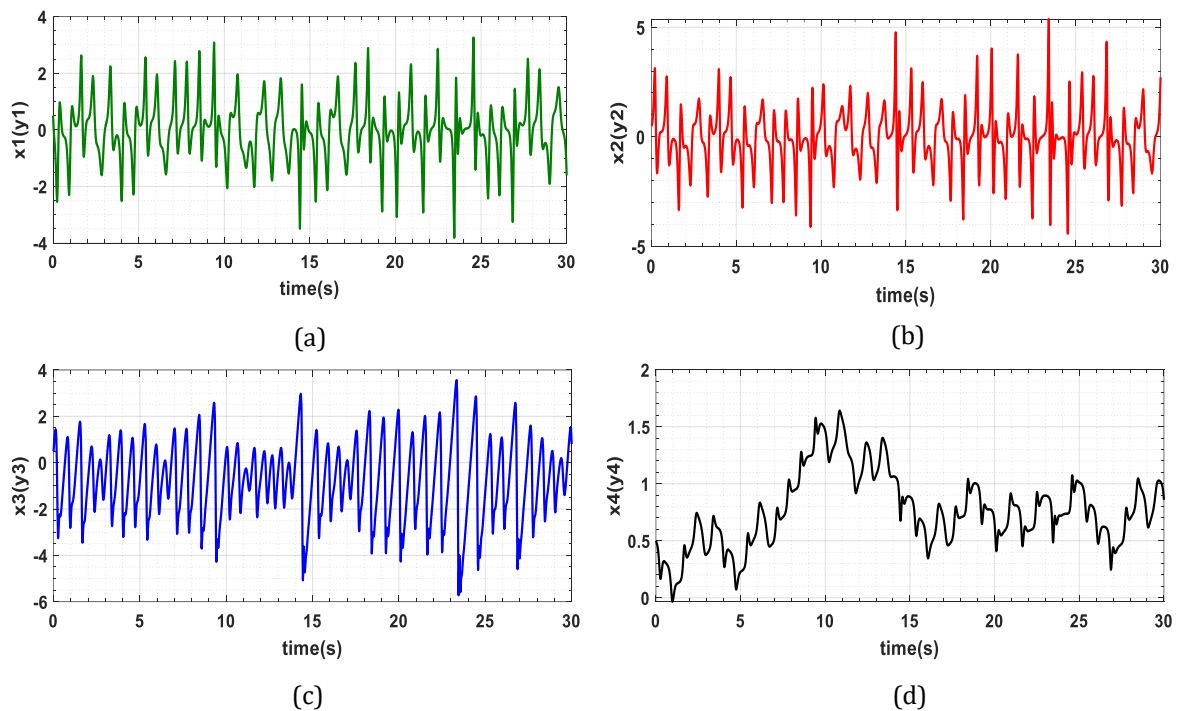


Fig. 2. State trajectories of the 4-D hyperchaotic system

3. Integral sliding mode controller and sliding surface design and analysis

In this section, we summarized the results for the global synchronization of the two hyperchaotic systems. Specifically, we obtained parameter ranges that assure the global stability of the system dynamics in the presence of known-parameter variations. The results can also be applied to the synchronization of non-identical systems.

Consider system (1) as the master system. Let the identical-parameter controlled slave system be represented in the form:

$$\begin{aligned}\dot{y}_1 &= -\alpha_1(y_1 + y_2) + \alpha_2 y_3 + u_{sm}^1 \\ \dot{y}_2 &= -\alpha_3 y_1 y_3 + \alpha_4 y_2 + \alpha_5 y_4 + u_{sm}^2 \\ \dot{y}_3 &= \alpha_6 y_1 y_2 + \alpha_7 + u_{sm}^3 \\ \dot{y}_4 &= -\alpha_8 y_1 - \alpha_9 y_2 - \alpha_{10} y_3 - \alpha_{11} y_4 + u_{sm}^4\end{aligned}\quad (2)$$

Where $u_{sm}^1, u_{sm}^2, u_{sm}^3$ and u_{sm}^4 are the ISMC laws to be derived, and y_1, y_2, y_3 and y_4 are state variables. Let the synchronization error between the master and slave systems be of the form:

$$e_i = y_i - x_i, \quad i = 1, 2, \dots, 4. \quad (3)$$

Given that the initial conditions of the master and slave systems, i.e., $x_i(0) \neq y_i(0)$, the coupled systems can be synchronized such that $\lim_{t \rightarrow \infty} \|e(t)\| = 0, \forall e_i$. The synchronization error system is given by

$$\begin{aligned}\dot{e}_1 &= -\alpha_1(e_1 + e_2) + \alpha_2 e_3 + u_{sm}^1 \\ \dot{e}_2 &= -\alpha_3(y_1 y_3 - x_1 x_3) - \alpha_4 e_2 - \alpha_5 e_4 + u_{sm}^2 \\ \dot{e}_3 &= \alpha_6(y_1 y_2 - x_1 x_2) + u_{sm}^3 \\ \dot{e}_4 &= -\alpha_8 e_1 - \alpha_9 e_2 - \alpha_{10} e_3 - \alpha_{11} e_4 + u_{sm}^4\end{aligned}\quad (4)$$

Synchronization of the systems involves two known steps viz: the selection of an appropriate switching surface which can guarantee the convergence of the system dynamics such that the error state dynamics asymptotically stabilizes in the sense of Lyapunov. Secondly, the derivation of suitable control law guarantees the existence of the sliding mode $s(t) = 0$. We define the integral sliding surface of each error state variable is defined as follows:

$$\begin{aligned}s_1 &= e_1 + \int_0^t \xi_1 e_1(\tau) d\tau \\ s_2 &= e_2 + \int_0^t \xi_2 e_2(\tau) d\tau \\ s_3 &= e_3 + \int_0^t \xi_3 e_3(\tau) d\tau \\ s_4 &= e_4 + \int_0^t \xi_4 e_4(\tau) d\tau\end{aligned}\quad (5)$$

The system trajectories glide on the sliding manifold if it satisfies the condition $\dot{s}_i = 0, (i = 1, 2, \dots, 4)$. Thus, differentiating (5) results in the following:

$$\begin{aligned}\dot{s}_1 &= \dot{e}_1 + \xi_1 e_1 \\ \dot{s}_2 &= \dot{e}_2 + \xi_2 e_2 \\ \dot{s}_3 &= \dot{e}_3 + \xi_3 e_3 \\ \dot{s}_4 &= \dot{e}_4 + \xi_4 e_4\end{aligned}\quad (6)$$

The Hurwitz condition is satisfied if $\xi_i (1, 2, \dots, 4)$ are positive constants. We set the following exponential reaching laws [22]

$$\begin{aligned}\dot{s}_1 &= -\gamma_1 \text{sgn}(s_1) - \Phi_1 s_1 \\ \dot{s}_1 &= -\gamma_1 \text{sgn}(s_1) - \Phi_1 s_1 \\ \dot{s}_2 &= -\gamma_2 \text{sgn}(s_2) - \Phi_2 s_2 \\ \dot{s}_3 &= -\gamma_3 \text{sgn}(s_3) - \Phi_3 s_3 \\ \dot{s}_4 &= -\gamma_4 \text{sgn}(s_4) - \Phi_4 s_4\end{aligned}\quad (7)$$

Where $\gamma_i > 0; \Phi_i > 0$ are positive constants to be determined. Comparing (6) and (7) gives

$$\begin{aligned}
\dot{e}_1 + \xi_1 e_1 &= -\gamma_1 \operatorname{sgn}(s_1) - \Phi_1 s_1 \\
\dot{e}_2 + \xi_2 e_2 &= -\gamma_2 \operatorname{sgn}(s_2) - \Phi_2 s_2 \\
\dot{e}_3 + \xi_3 e_3 &= -\gamma_3 \operatorname{sgn}(s_3) - \Phi_3 s_3 \\
\dot{e}_4 + \xi_4 e_4 &= -\gamma_4 \operatorname{sgn}(s_4) - \Phi_4 s_4
\end{aligned} \tag{8}$$

By inserting (4) into (8), we have

$$\begin{aligned}
-\alpha_1(e_1 + e_2) + \alpha_2 e_3 + \xi_1 e_1 + u_{sm}^1 &= -\gamma_1 \operatorname{sgn}(s_1) - \Phi_1 s_1 \\
-\alpha_3(y_1 y_3 - x_1 x_3) - \alpha_4 e_2 - \alpha_5 e_4 + \xi_2 e_2 + u_{sm}^2 &= -\gamma_2 \operatorname{sgn}(s_2) - \Phi_2 s_2 \\
\alpha_6(y_1 y_2 - x_1 x_2) + \xi_3 e_3 + u_{sm}^3 &= -\gamma_3 \operatorname{sgn}(s_3) - \Phi_3 s_3 \\
-\alpha_8 e_1 - \alpha_9 e_2 - \alpha_{10} e_3 - \alpha_{11} e_4 + \xi_4 e_4 + u_{sm}^4 &= -\gamma_4 \operatorname{sgn}(s_4) - \Phi_4 s_4
\end{aligned} \tag{9}$$

3.1. Theorem

If the following ISMC laws (10) are applied to the master and slave systems (1) and (2) for all initial conditions $x_i(0)$, ($i = 1, 2, \dots, 4$) $\neq y_i(0)$, ($i = 1, 2, \dots, 4$), then error state dynamics will asymptotically converge on the sliding surface $s(t) = 0$ in the sense of Lyapunov, i.e. $\lim_{t \rightarrow \infty} \|e(t)\| = 0, \forall e_i$. Furthermore, the coupled dynamics of the master-slave systems are completely synchronized as $t \rightarrow \infty, \forall x_i(0), (i = 1, 2, \dots, 4) \neq y_i(0), (i = 1, 2, \dots, 4)$.

$$\begin{aligned}
u_{sm}^1 &= \alpha_1(e_1 + e_2) - \alpha_2 e_3 - \xi_1 e_1 - \gamma_1 \operatorname{sgn}(s_1) - \Phi_1 s_1 \\
u_{sm}^2 &= \alpha_3(y_1 y_3 - x_1 x_3) + \alpha_4 e_2 + \alpha_5 e_4 - \xi_2 e_2 - \gamma_2 \operatorname{sgn}(s_2) - \Phi_2 s_2 \\
u_{sm}^3 &= -\alpha_6(y_1 y_2 - x_1 x_2) - \xi_3 e_3 - \gamma_3 \operatorname{sgn}(s_3) - \Phi_3 s_3 \\
u_{sm}^4 &= \alpha_8 e_1 + \alpha_9 e_2 + \alpha_{10} e_3 + \alpha_{11} e_4 - \xi_4 e_4 - \gamma_4 \operatorname{sgn}(s_4) - \Phi_4 s_4
\end{aligned} \tag{10}$$

Proof:

Based on the Lyapunov stability theory [30], we consider a quadratic Lyapunov function candidate given as follows:

$$V(s_1, s_2, s_3, s_4) = \frac{1}{2}(s_1^2 + s_2^2 + s_3^2 + s_4^2) \tag{11}$$

where V is positive definite on R^4 . Through partial derivative, (11) is transformed

$$\dot{V}(s_1, s_2, s_3, s_4) = s_1 \dot{s}_1 + s_2 \dot{s}_2 + s_3 \dot{s}_3 + s_4 \dot{s}_4 \tag{12}$$

By inserting (7) in (12) and using the convention $s_1 \operatorname{sgn}(s_1) = |s_1|$, we have

$$\dot{V}(s_1, s_2, s_3, s_4) = -\gamma_1 |s_1| - \xi_1 s_1^2 - \gamma_2 |s_2| - \xi_2 s_2^2 - \gamma_3 |s_3| - \xi_3 s_3^2 - \gamma_4 |s_4| - \xi_4 s_4^2 \tag{13}$$

Equation (13) is negative definite on R^4 . Thus, the theorem is satisfied, and the trajectories of the synchronization error dynamics will asymptotically converge to the origin because $\dot{V} \leq 0$ and this also implies that $V(\dot{0}) \leq 0$. Compactly, (13) can be rendered in the form

$$\dot{V}(s_1, s_2, s_3, s_4) = \sum_{i=1}^4 s_i (-\gamma_i \operatorname{sgn}(s_i) - \xi_i s_i) \tag{14}$$

4. Numerical simulation results

MATLAB 2019a provided the numerical simulation environment. Initial conditions of the master and slave systems are $[x_1(0), x_2(0), x_3(0), x_4(0)] = [5, 8, 10, 15]$ and $[y_1(0), y_2(0), y_3(0), y_4(0)] = [15, 14, 13, 10]$; $\gamma_1 = \gamma_2 = \gamma_3 = \gamma_4 = 0.01$; $\xi_1 = \xi_2 = \xi_3 = \xi_4 = 1$ and $\Phi_1 = \Phi_2 = \Phi_3 = \Phi_4 = 20$. For the sliding surface, $s_1(0) = s_2(0) = s_3(0) = s_4(0) = 1$. Fig. 3, Fig. 4, Fig. 5, Fig. 6, Fig. 7, and Fig. 8 are the results of the simulation.

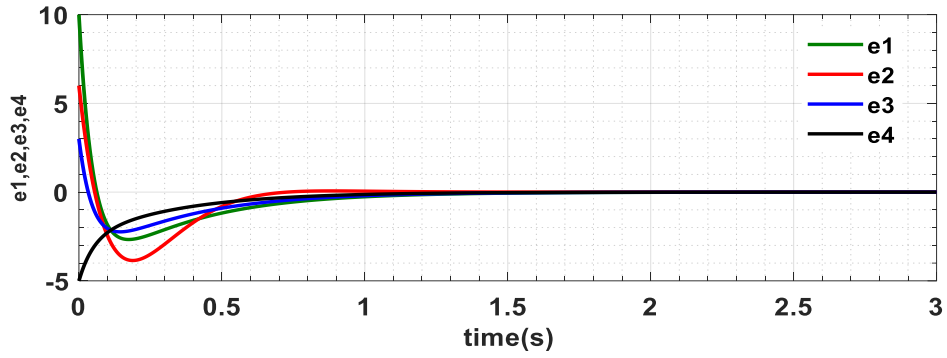


Fig. 3. Asymptotically-converged dynamics of the synchronization error

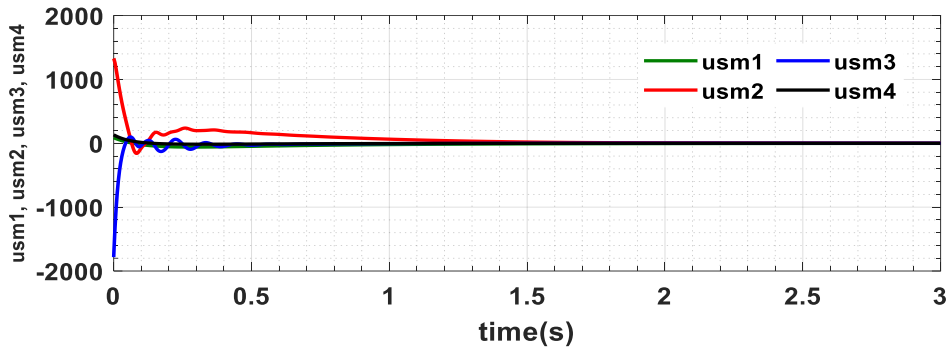


Fig. 4. Asymptotically-converged dynamics of the ISMC laws

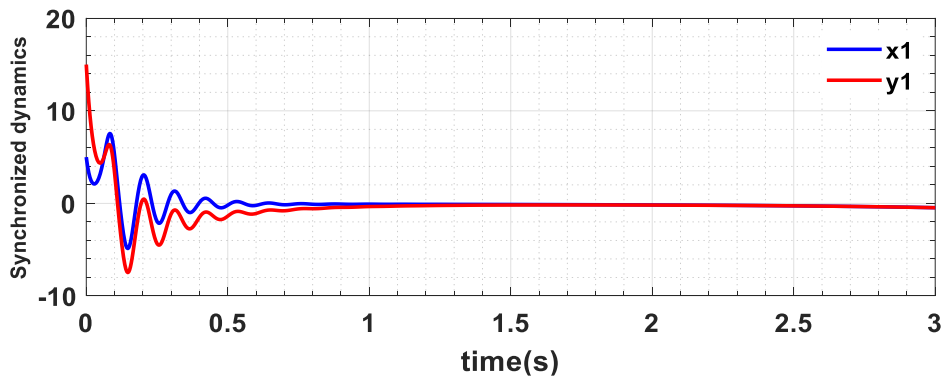


Fig. 5. Synchronized dynamics of state trajectories of x_1 and y_1

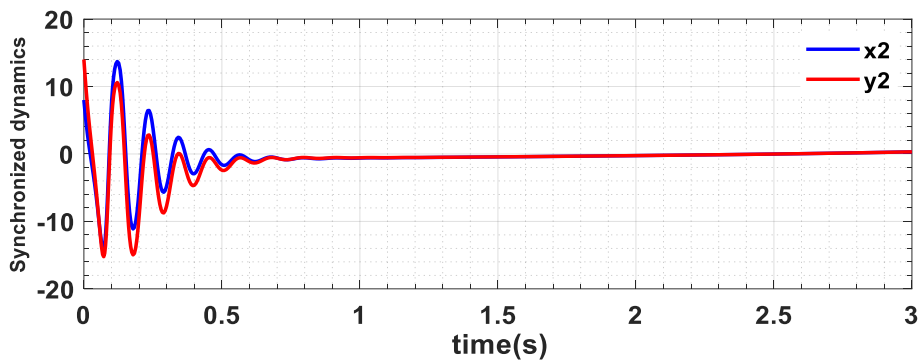


Fig. 6. Synchronized dynamics of state trajectories of x_2 and y_2

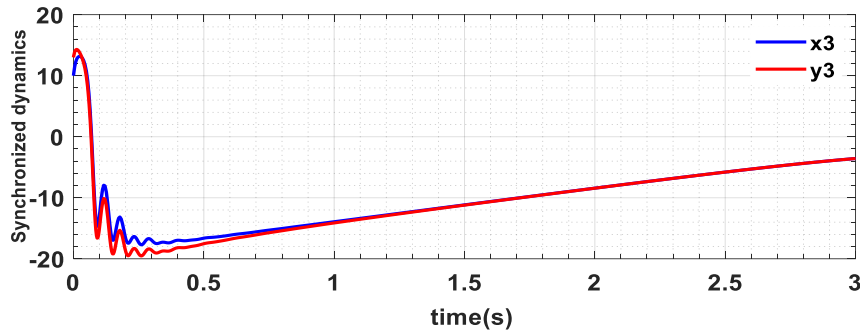


Fig. 7. Synchronized dynamics of state trajectories of x_3 and y_3

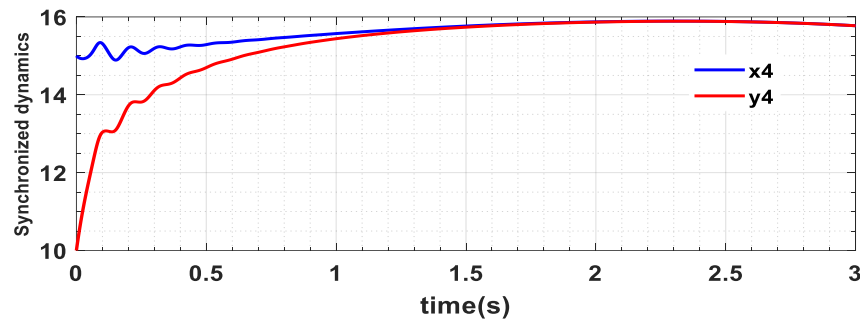


Fig. 8. Synchronized dynamics of state trajectories of x_4 and y_4

4.1. Robustness test via parameter variation

In the section, the parameters of the systems were varied to evolve a topologically non-equivalent case. The resulting plots of the converged error state and controller dynamics are shown in Fig. 9 and Fig. 10.

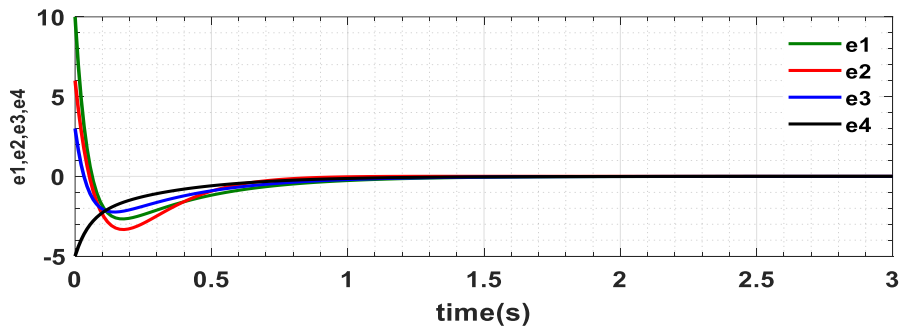


Fig. 9. Asymptotically-converged dynamics of the synchronization error states

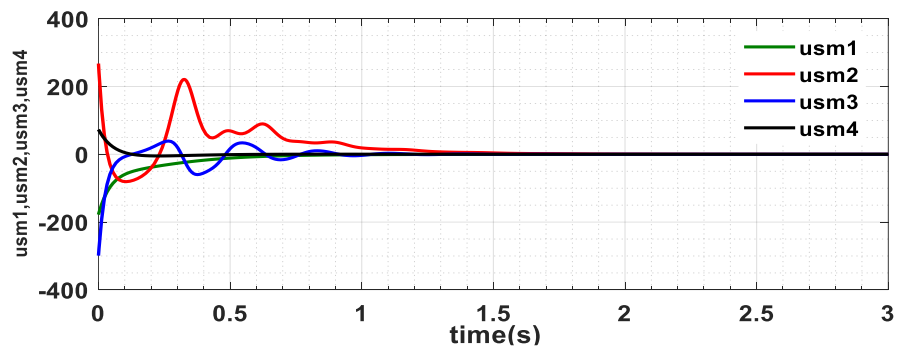


Fig. 10. Asymptotically-converged dynamics of the ISMC laws

4.2. Discussion

When the ISMC laws are applied according to the architecture in Fig. 1, the synchronization error dynamics converged asymptotically, as shown in Fig. 3. The ISMC laws asymptotically converged to the origin in the sense of Lyapunov. Furthermore, each of the state trajectories of the identical master and slave systems in Fig. 2 (a) – (d) were synchronized as shown in Fig. 5 – Fig. 8. The test of robustness based on known-parameters variation using the ISMC laws resulted in the error state trajectories depicted in Fig. 9 and converged ISMC laws depicted in Fig. 10. It can be seen from Fig. 9 and Fig. 10 that the controller is invariant in the presence of parameter variation. This fact can be extended to the case of parameter uncertainty of the slave system.

5. Conclusion and Future Work

In this paper, integral sliding mode control laws were derived from synchronizing the state trajectories of identical 4-D hyperchaotic systems based on the Lyapunov stability principle. The control laws were observed to be invariant to known-parameter variations of the system during robustness tests. As an open problem, the synchronization of chaotic systems continues to hold promises for applications in robotic motion control, electric drive system, and other traction control systems. The modeled ISMC laws can be improved upon so that the transient time that elapsed before coupling can be finite-time (i.e., precisely determined) for applications in time-critical dynamic systems.

Funding: This research received no external funding.

Conflicts of Interest: The authors declare no conflict of interest.

References

- [1] E. A. Umoh, "Synchronization of chaotic flows with variable nonlinear hyperbolic functions via hybrid feedback control," *Proceedings of the 2nd Pan African International Conference on Science, Computing and Telecommunications (PACT 2014)*, 2014, pp. 7–11. <https://doi.org/10.1109/SCAT.2014.7055126>
- [2] V. I. Utkin, "Survey paper on variable structure systems with sliding modes," *IEEE Trans. Automat. Contr.*, vol. 22, no. 2, pp. 212–222, 1977. <https://doi.org/10.1109/TAC.1977.1101446>
- [3] Y. Pan, C. Yang, L. Pan, and H. Yu, "Integral sliding mode control: performance, modification and improvement," *IEEE Trans. Ind. Informatics*, 2018. <https://doi.org/10.1109/TII.2017.2761389>
- [4] A. Chalanga, S. Kamal, L. M. Fridman, B. Bandyopadhyay, and J. A. Moreno, "Implementation of super-twisting control: Super-twisting and higher order sliding-mode observer-based approaches," *IEEE Trans. Ind. Electron.*, vol. 63, no. 6, pp. 3677–3685, 2016. <https://doi.org/10.1109/TIE.2016.2523913>
- [5] N. B. Ammar, S. Bouallegue, J. Hagege, and S. Vaidyanathan, "Chattering Free Sliding Mode Controller Design for a Quadrotor Unmanned Aerial Vehicle," *Applications of Sliding Mode Control in Science and Engineering*, 2017, pp. 81–98. https://doi.org/10.1007/978-3-319-55598-0_3
- [6] P. A. Hosseinabadi, A. S. S. Abadi, S. Mekhilef, and H. R. Pota, "Two novel approaches of adaptive finite-time sliding mode control for a class of single-input multiple-output uncertain nonlinear systems," *IET Cyber-Systems Robot.*, vol. 3, no. 2, pp. 173–183, 2021. <https://doi.org/10.1049/csy2.12012>
- [7] M. S. Mahmoud and A. H. AlRamadhan, "Optimizing the parameters of sliding mode controllers for stepper motor through Simulink response optimizer application," *Int. J. Robot. Control Syst.*, vol. 1, no. 2, pp. 209–225, 2021. <https://doi.org/10.31763/ijrcs.v1i2.345>
- [8] M. S. Mahmoud, A. Alameer, and M. M. Hamdan, "An adaptive sliding mode control for single machine infinite bus system under unknown uncertainties," *Int. J. Robot. Control Syst.*, vol. 1, no. 3,

- pp. 226–243, 2021. <https://doi.org/10.31763/ijrcs.v1i3.351>
- [9] J. Baek, M. Jin, and S. Han, “A New adaptive sliding mode control scheme for application to robot manipulators,” *IEEE Trans. Ind. Electron.*, vol. 63, no. 6, pp. 3628–3637, 2016. <https://doi.org/10.1109/TIE.2016.2522386>
- [10] H. Sira-Ramírez, M. A. Aguilar-Orduña, and E. W. Zurita-Bustamante, “On the sliding mode control of MIMO nonlinear systems: An input-output approach,” *Int. J. Robust Nonlinear Control*, vol. 29, no. 3, pp. 715–735, 2019. <https://doi.org/10.1002/rnc.4320>
- [11] C.-K. Lai, B.-W. Lin, H.-Y. Lai, and G.-Y. Chen, “FPGA-based hybrid stepper motor drive system design by variable structure control,” *Actuators*, vol. 10, no. 6, p. 113, 2021. <https://doi.org/10.3390/act10060113>
- [12] K. Lochan, J. P. Singh, and K. R. Binoy, “Tracking control and deflection suppression of an AMM modelled TLFM using backstepping based adaptive SMC technique,” *Control Instrumentation Systems*, 2020, pp. 43–58. https://doi.org/10.1007/978-981-13-9419-5_4
- [13] A. Norouzi, M. Masoumi, A. S. Barari, and F. Saina, “Lateral control of an autonomous vehicle using integrated backstepping and sliding mode controller,” *J. Multi-body Dyn.*, vol. 233, no. 1, pp. 141–151, 2019. <https://doi.org/10.1177/1464419318797051>
- [14] P. P. Singh, J. P. Singh, and B. K. Roy, “SMC based synchronization and anti- synchronization of chaotic systems for secure communication and analog circuit realization,” *Int. J. Control Theory Appl.*, vol. 9, no. 39, pp. 171–183, 2016. <https://www.researchgate.net/profile/Jay-Singh-17/publication/313397806>
- [15] S. Mobayen, “A Novel global sliding mode control based on exponential reaching law for a class of underactuated systems with external disturbances,” *J. Comput. Nonlinear Dyn.*, vol. 11, pp. 021011-1–11, 2016. <https://doi.org/10.1115/1.4031087>
- [16] K. B. Devika and S. Thomas, “Power rate exponential reaching law for enhanced performance of sliding mode control,” *Int. J. Control. Autom. Syst.*, vol. 15, no. 6, pp. 2636–2645, 2017. <http://dx.doi.org/10.1007/s12555-016-0736-9>
- [17] M. Monsalve-Rueda, J. Candelo-Becerra, and F. Hoyos, “Dynamic behavior of a sliding-mode control based on a washout filter with constant impedance and nonlinear constant power loads,” *Appl. Sci.*, vol. 9, p. 4548, 2019. <http://dx.doi.org/10.3390/app9214548>
- [18] M. Fathallah, F. Abdelhedi, and N. Derbel, “Insensibility of the second order sliding mode control via measurement noises: Application to a robot manipulator surveillance camera,” *Applications of Sliding Mode Control in Science and Engineering*, 2017, pp. 99–113. https://doi.org/10.1007/978-3-319-55598-0_5
- [19] S. Roy, S. Baldi, and L. M. Fridman, “On adaptive sliding mode control without a priori bounded uncertainty,” *Automatica*, vol. 111, p. 108650, 2020. <http://dx.doi.org/10.1016/j.automatica.2019.108650>
- [20] V. I. Utkin and S. Jingxin, “Integral sliding mode in systems operating under uncertain conditions,” *Proceedings of 35th IEEE Conference on Decision and Control*, 1996, pp. 4591–4596. <https://doi.org/10.1109/CDC.1996.577594>
- [21] Y. Guo, B. Huang, A.-J. Li, and C.-Q. Wang, “Integral sliding mode control for Euler-Lagrange systems with input saturation,” *Int. J. Robust Nonlinear Control*, vol. 29, pp. 1088–1100, 2019. <https://doi.org/10.1002/rnc.4431>
- [22] A. Sambas, S. Vaidyanathan, M. M. Sudarno, and M. A. Mohamed, “Investigation of chaos behavior in a new two-scroll chaotic system with four unstable equilibrium points, its synchronization via four control methods and circuit simulation,” *IAENG Int. J. Appl. Math.*, vol. 50, no. 1, 2020. http://www.iaeng.org/IJAM/issues_v50/issue_1/IJAM_50_1_03.pdf
- [23] C.-H. Lin and F.-Y. Hsiao, “Proportional-integral sliding mode control with an application in the balance control of a two-wheel vehicle system,” *Appl. Sci.*, vol. 10, p. 27pp, 2020. <https://doi.org/10.3390/app10155087>
- [24] H. D. Tho, R. Tasaki, A. Kaneshige, T. Miyoshi, and K. Terashima, “Robust sliding mode control with integral sliding surface of an underactuated rotary hook system,” *2017 IEEE International Conference on Advanced Intelligent Mechatronics (AIM)*, 2017, pp. 998–1003. <https://doi.org/10.1109/AIM.2017.8014149>

- [25] E. A. Umoh and O. N. Iloanusi, "Algebraic structure, dynamics and electronic circuit realization of a novel reducible hyperchaotic system," *2017 IEEE 3rd International Conference on Electro-Technology for National Development (NIGERCON 2017)*, 2017, pp. 483–490. <https://doi.org/10.1109/NIGERCON.2017.8281917>
- [26] E. A. Umoh and O. N. Iloanusi, "Visualization and heuristic optimization of bifurcation scenarios of a 4D hyperchaotic flow," *2nd International Conference on ICT and its Applications (ICTA 2018)*, 2018, pp. 503–507. <https://www.researchgate.net/profile/Edwin-Umoh/publication/328433742>
- [27] E. A. Umoh and O. N. Iloanusi, "Chaotic analysis and improved finite-time adaptive stabilization of a novel 4-D hyperchaotic system," *Adv. Syst. Sci. Appl.*, vol. 18, no. 4, pp. 121–35, 2018. <https://doi.org/10.25728/assa.2018.18.4.623>
- [28] E. A. Umoh, O. N. Iloanusi, and U. A. Nnolim, "Image multi-encryption architecture based on hybrid keystream sequence interspersed with Haar discrete wavelet transform," *IET Image Process.*, vol. 14, no. 10, 2020. <https://doi.org/10.1049/iet-ipr.2019.0991>
- [29] E. A. Umoh and O. N. Iloanusi, "Robustness analysis of a hyperchaos-based digital image encryption algorithm under noise attacks," *Int. J. Eng. Res. Africa*, vol. 43, pp. 71–83, 2019. <https://doi.org/10.4028/www.scientific.net/JERA.43.71>
- [30] H. K. Khalil, *Nonlinear Systems*, 2nd ed. New Jersey: Prentice Hall Inc., 1996. https://books.google.co.id/books/about/Nonlinear_Systems.html?id=t_d1QgAACAAJ&redir_esc=y